Journal of Marine Research, 64, 629–650, 2006

A model of methane concentration profiles in the open ocean

by G. C. Nihous[1,2] and S. M. Masutani[1]

ABSTRACT

Methane-bearing particulate matter formed in the upper ocean layer is allowed to settle and degrade, releasing methane into the water column as a source in one-dimensional advection-diffusion equations. Predicted carbon and methane particulate fluxes are in good agreement with sediment trap data, using parameters of expected magnitude and particulate methane production well within the mixed layer. This suggests a rapid pathway to the atmosphere and reduced effects on methane concentrations below. Vertical advection rates yielding a good fit between methane concentration calculations and data are larger than expected unless methane oxidation is included. This confirms the significance of methane oxidation in shaping open-ocean methane concentration profiles in spite of turnover times of decades. Predictions of the isotopic composition of dissolved methane $\delta^{13}C$ with the one-dimensional model are more difficult, although trends in measured vertical profiles can be reproduced. While this work does not shed light on the purported mechanism of methane *generation* in the upper ocean, it shows that methane of particulate origin is sufficient to explain observed open-ocean methane concentrations.

1. Introduction

The measurement of methane concentration profiles in the open ocean has been the focus of significant interest for the oceanographic research community, even though this species is present at nanomolar levels (Burke *et al.,* 1983; Ward *et al.,* 1987; Conrad and Seiler, 1988; Karl and Tilbrook, 1994; Tilbrook and Karl, 1995; Watanabe *et al.,* 1995; Holmes *et al.,* 2000; Sansone *et al.,* 2001). An important feature of the data is the consistent and widespread supersaturation of surface waters with methane relative to the atmosphere, which results in the oceans being a source of this greenhouse gas (IPCC, 2001).[3] Methane concentrations are observed to substantially taper off with increasing water depth. The existence of a net methane flux from the open ocean to the atmosphere is puzzling since potential methanogenic processes in seawater are known to be anaerobic. A credible explanation rests on the existence of anaerobic microniches in oxic surface waters. Karl

1. Hawaii Natural Energy Institute, School of Ocean and Earth Science and Technology, University of Hawaii, Honolulu, Hawaii, 96822, U.S.A.

2. Corresponding author. ***email: nihous@hawaii.edu***

3. For an updated overview of the global methane biogeochemical cycle, readers are referred to Reeburgh (2003).

and Tilbrook (1994) and Tilbrook and Karl (1995) suggested that the most likely site for *in situ* methane generation are zooplankton guts, where high rates of oxygen consumption would promote methanogenesis. They also favored the diffusive loss pathway from egested particulate matter to the water column as the most probable, while not excluding other mechanisms like particle disaggregation.

The primary goal of this paper is to test Karl and Tilbrook's (1994) hypothesis that '*. . . methane is formed in zooplankton guts and enters the sinking particle field through the process of faecal pellet formation.*' To this end, a simple one-dimensional physical model of the phenomena that would follow '*pellet formation*' is proposed in the following Section. Calculations are then performed and compared with available field data.

2. Model description

The phenomena of interest are assumed to have reached a steady-state and to exhibit negligible variability in the horizontal direction. The latter point justifies a one-dimensional vertical model. Cases being investigated rely on the collection of specific data in order to test the connection between methane of particulate origin and methane dissolved in the water column. While the seawater methane concentration u must be known, it is not sufficient *per se;* one also needs information that can be related to methane in particulate form. A review of the literature indicates that, although u has been extensively measured, there currently are only a very limited number of 'complete' data sets that also include the necessary particulate measurements. The model developed here was applied to the general open-ocean region northeast of the Hawaiian Islands because profiles for u, estimates of the ocean-atmosphere methane flux $F_{CH_4}(L)$ as well as sediment trap measurements of the particulate organic carbon (POC) flux τ and particulate methane flux τ_{CH_4} were available.

The general modeling approach is illustrated in Figure 1. The particulate and dissolved methane problems are treated separately on the premise that the sinking of methane-bearing particulate matter overwhelms other transport mechanisms such as turbulent diffusion and advection. The solution of the particulate problem is constrained by field data on $F_{CH_4}(L)$, τ and τ_{CH_4}. This solution yields a source term S representing the transfer of methane from particulate matter to the water column. S is a fundamental input to an advection-diffusion equation for u, and therefore represents the primary connection between the two problems.

a. General relationships

The model employs a one-dimensional vertical coordinate system x which has its origin on the seafloor. The ocean surface is located at $x = L$. The production of particulate organic carbon (POC) $P(x)$ also containing a small amount of methane is postulated. The ratio of particulate methane to POC in the source term P is r_0. It is assumed that the particulate matter sinks with velocity $W < 0$. We define $p(x; \xi)$ as the POC source at x

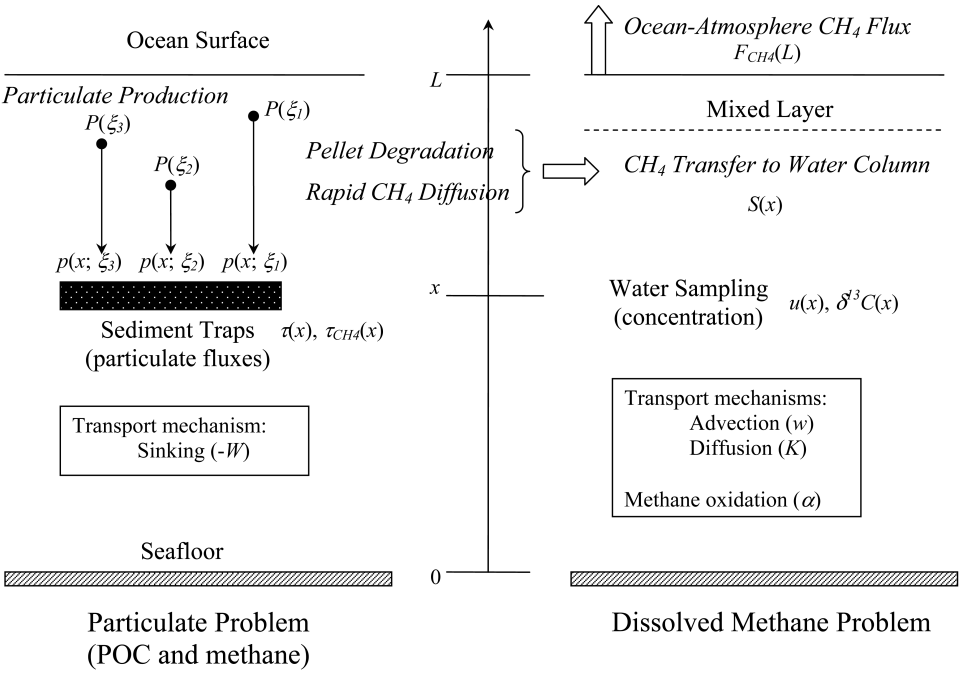

Figure 1. Schematic diagram of overall modeling approach

resulting from production at ξ. In what follows, a subscript CH_4 will define physical quantities for methane, e.g., $p_{CH_4}(x; \xi)$. Assuming that there is no particulate source from the atmosphere, the downward POC flux resulting from production in the water column is:

$$\tau = \int_x^L p(x; \xi) d\xi. \tag{1}$$

A mass balance on an elementary slab of thickness dx can be written:

$$\frac{d\tau}{dx} = S(x) - P(x) \tag{2}$$

where $S(x)$, as discussed previously, represents the dissolved organic carbon (DOC) source associated with any transfer of carbon from the particulate matter into the water column at x. Differentiating Eq. (1) with respect to x and substituting in Eq. (2) yields:

$$S = \int_x^L \frac{\partial p}{\partial x}(x; \xi) d\xi. \tag{3}$$

Use has been made of the identity $p(x; x) = P(x)$. Finally, Tillbrook and Karl (1994) define a methane-to-carbon ratio for particulate matter at any location as $r = \tau_{CH_4}/\tau$.

Integrating Eq. (2) for methane from 0 to L next yields:

$$-\tau_{CH_4}(0) = \int_0^L S_{CH_4}(\xi)d\xi - \int_0^L r_0 P(\xi)d\xi. \tag{4}$$

Calling the upward flux of dissolved methane through the water column F_{CH_4}, it is equal to $F_{CH_4}(0) + \int_0^x S_{CH_4}(\xi)d\xi$ in the absence of other sources and sinks (or if those are negligible). Eq. (4) then may be written:

$$\int_0^L r_0 P(\xi)d\xi = \tau_{CH_4}(0) + F_{CH_4}(L) - F_{CH_4}(0) \tag{5}$$

b. Estimation of particulate sources p(x; ξ) and $p_{CH_4}(x; \xi)$

We assume that the magnitude of the sinking velocity of the 'pellets' carrying the particulate matter is large enough to overwhelm turbulent diffusion and vertical advection. With the formula of Dietrich (1982), we can estimate $-W$; for example, pellets 150 μm in diameter with a relative excess density of 0.01 to 0.1 would sink at about 0.12 to 1.2 mm/s. In comparison, vertical advection typically is three to four orders of magnitude smaller (Stommel, 1958; Munk, 1966; Huang, 1992; Hodnett and McNamara, 2000).

The evolution of the pellets originating at $x = \xi$ occurs by degradation, as defined in ecological models with a coefficient A (Kawamiya *et al.,* 1995; Kishi *et al.,* 2001; Yanagi *et al.,* 2001), and by diffusion of methane into the water column. Tilbrook and Karl (1994) reported ratios r less than 1 μmol-CH_4/mmol-C; therefore, the diffusion of methane out of the pellets should have no significant effect on the POC budget. We can write:

$$\frac{dp}{p} = -\frac{A}{W}dx. \tag{6}$$

The boundary condition simply is $p(\xi, \xi) = P(\xi)$, and the equation holds for $x \leq \xi$. Defining a degradation length scale $\bar{X} = -$W/A, which we assume to be independent of x, Eq. (6) can be integrated with respect to x:

$$p(x; \xi) = P(\xi)\exp\left\{\frac{x - \xi}{\bar{X}}\right\}. \tag{7}$$

With A of the order of 0.05 per day (Kawamiya *et al.,* 1995; Kishi *et al.,* 2001; Yanagi *et al.,* 2001), $\bar{X}$ should be of the order of hundreds of meters.

The case of $p_{CH_4}(x; \xi)$ is more complex. We first envision the diffusive transfer of methane out of the pellets to proceed at a rate sHC_0, where s is the exchange surface area per cubic meter per unit time associated with P; H a mass transfer coefficient (dimension-

ally, a velocity); and C_0 represents the methane concentration inside the pellets (assumed to be much larger than water-column concentrations). We then have:

$$\frac{dp_{CH4}}{dx} = -\frac{sHC_0}{W} + \frac{p_{CH4}}{\bar{X}}. \tag{8}$$

Jumars *et al.* (1989) argued that most highly concentrated solutes in small fecal pellets diffuse very rapidly into the water column. The precise structure of pellets and the pathway for diffusion, however, are not well known. To make the problem formulation flexible, we define a diffusive length scale $\bar{x}$ as the distance over which a fraction η of the initial methane content (r_0P) in the pellets is rapidly released in the water column, independently of pellet degradation. In other words, $\bar{x} = -\eta r_0 PW/(sHC_0)$. To be consistent with Jumars *et al.* (1989), η should be high (e.g., 90%) and $\bar{x}$ rather small, of the order of meters to tens of meters. Eq. (8) may be recast as:

$$\frac{dp_{CH4}}{dx} = \frac{\eta r_0 P}{\bar{x}} + \frac{p_{CH4}}{\bar{X}}. \tag{9}$$

The boundary condition is $p_{CH_4}(\xi, \xi) = r_0P(\xi)$, and the equation holds for $x \leq \xi$. Assuming that $\bar{x}$ is independent of x and postulating that the fraction η only is released via diffusion, we can integrate Eq. (9) as follows:

$$\begin{cases} p_{CH_4}(x;\,\xi) = r_0P(\xi)\left\{1 + \dfrac{\eta\bar{X}}{\bar{x}}\right\}\exp\left\{\dfrac{x-\xi}{\bar{X}}\right\} - \dfrac{\eta r_0 \bar{X} P(\xi)}{\bar{x}} & \text{for } \xi - \bar{\bar{x}} \leq x \leq \xi \quad (10a) \\ p_{CH_4}(x;\,\xi) = (1-\eta) r_0 P(\xi)\,\dfrac{1+\eta\,\dfrac{\bar{X}}{\bar{\bar{x}}}}{1+\eta\left(\dfrac{\bar{X}}{\bar{x}}-1\right)}\exp\left\{\dfrac{x-\xi}{\bar{X}}\right\} & \text{for } x \leq \xi - \bar{\bar{x}} \quad (10b) \end{cases}$$

$\bar{\bar{x}}$ is the diffusive length scale corrected for pellet degradation; it corresponds to the condition $p_{CH_4}(\xi - \bar{\bar{x}};\, \xi) = (1 - \eta) r_0 P(\xi)$. Thus, $\bar{\bar{x}} = \bar{X}\,\mathrm{Log}\{1 + \eta/(1 + \eta[\bar{X}/\bar{x} - 1])\}$.

c. Methane concentrations in the water column

The transport mechanisms affecting dissolved methane in the water column are turbulent diffusion and advection. Methane may also be removed by methane oxidation which is usually represented as a first-order reaction with specific rate α. When the vertical diffusion coefficient K and upward advection rate w are constant, a methane mass balance on an elementary slab of thickness dx yields the following ordinary differential equation for the methane concentration u:

$$-K\frac{d^2u}{dx^2} + w\frac{du}{dx} + \alpha u = S_{CH_4} \tag{11}$$

The right-hand side methane source from particulate matter can be determined from Eq. (3) and Eq. (10). To simplify the analysis, an upper boundary condition $u = u_m$ is adopted where u_m is the methane concentration in a mixed layer of thickness h_m. A typical value $h_m = 75$ m (Li *et al.,* 1984) is adopted for all calculations. Eq. (11) then is only solved in the domain $0 > x > L - h_m$. A secondary boundary condition $u = u_0$ is imposed on the seafloor. u_0 is a representative abyssal methane concentration and is nonzero, as reported in Scranton and Brewer (1978); Holmes *et al.* (2000), e.g., for the July 1997 data; and Watanabe *et al.* (1995). Numerically, Eq. (11) was solved with a straightforward fourth-order Runge-Kutta scheme.

The somewhat idealized one-dimensional representation of ocean water-column characteristics with constant upward advection velocity and vertical diffusion coefficient has been popular (Stommel, 1958; Munk, 1966). Although simplistic, it leads, for example, to realistic temperature profiles; the use of an 'overall diffusion coefficient' K only, as in Li *et al.* (1984), does not adequately reproduce the thermocline. More advanced three-dimensional models of oceanic circulation allow for vertical advection rates that vary with depth, among other things (Huang, 1992; Hodnett and McNamara, 2000).

The consideration of $w(x)$ in a one-dimensional model is attractive because it allows a limited representation of real phenomena such as Ekman pumping and barotropic ventilation (when isopycnal surfaces are not horizontal). In this case, a water mass balance on an elementary slab of thickness dx can only be achieved with a pseudo-source dw. It can be verified that the effect of this pseudo-source on the mass balance of a tracer like methane is to preserve the form of Eq. (11) when w is a function of x.

In the central North Pacific Subtropical Gyre (NPSG), the upper layer experiences substantial downwelling from Ekman pumping, at rates of about 30 m per year (Winn *et al.,* 1994); in the eastern part of the NPSG, there is subduction of heavier Northern waters as well (Flament *et al.,* 1997). Three-dimensional calculations of ocean circulation confirm the prevalence of upper-ocean downwelling in this region (Pierce, 2004). Thus, a surface value $w_e = w(L)$ of the order of -1.0×10^{-6} m/s is quite realistic for the general area where there is sufficient data on methane concentration and particulate matter for the model developed in this paper to be tested. Adapting the two-layer model of Huang (1992), we further considered a function $w(x)$ that grows linearly from 0 at the seafloor to a positive value w_{tr} at the top of an abyssal layer of 3500 m. In the upper layer of thickness $H_{up} = 500$ m, $w(x)$ is a parabolic function determined by $w(L) = w_e$, $w(L - H_{up}) = w_{tr}$ and the continuity of dw/dx at $x = L - H_{up}$.

d. Isotopic carbon composition of methane in the water column

Calling R the isotopic ratio $^{13}C/^{12}C$ in methane, isotopic composition is described by $\delta^{13}C(‰) = 1000\{R/R_{PDB} - 1\}$, where R_{PDB} is the isotopic ratio of the PDB standard equal to 0.011237 (Craig, 1957). An equation similar to Eq. (11) can be derived for the concentration of $^{13}CH_4$ in the water column, ^{13}u. $\delta^{13}C(‰)$ is related to ^{13}u via the identity $R = {}^{13}u/(u - {}^{13}u)$.

We assume that no isotopic fractionation is associated with turbulent diffusion, advection or the mechanisms driving the transfer of methane from particulate matter into the water column. If $\delta^{13}C_{new}$ is the isotopic composition of methane in the particulate matter, the $^{13}CH_4$ flux into the water column then is $S_{CH_4}\{R_{new}/(1 + R_{new})\}$ where $R_{new} = R_{PDB}(1 + \delta^{13}C_{new}10^{-3})$. Isotopic fractionation occurs with microbial methane oxidation (Barker and Fritz, 1981; Coleman *et al.,* 1981). The associated fractionation factor α_k is the ratio of ambient isotopic ratio over the isotopic ratio of methane removed during oxidation:

$$\alpha_k = \frac{^{13}u(u - {}^{13}u_{ox})}{^{13}u_{ox}(u - {}^{13}u)} \tag{12}$$

$^{13}u_{ox}$ is defined as the $^{13}CH_4$ concentration in methane used in the first-order-reaction sink αu. Eq. (12) yields:

$$^{13}u_{ox} = \frac{u\,{}^{13}u}{^{13}u + \alpha_k(u - {}^{13}u)} \tag{13}$$

α_k is slightly larger than one while $u \gg {}^{13}u$ so that $^{13}u_{ox} \approx {}^{13}u/\alpha_k$.

The differential equation describing the evolution of ^{13}u can now be written as:

$$-K\frac{d^2(^{13}u)}{dx^2} + w\frac{d(^{13}u)}{dx} + \alpha\,{}^{13}u_{ox} = \frac{R_{new}S_{CH_4}}{1 + R_{new}}. \tag{14}$$

Two boundary conditions must be provided. Unless the approximation $^{13}u_{ox} \approx {}^{13}u/\alpha_k$ is made, the methane concentration u must first be calculated.

3. Results and discussion

a. Production functions P(x) and $r_0P(x)$

We consider particulate methane production occurring on the average at a rate r_0P_0 over a layer λ, so that $\int_0^L r_0P(\xi)d\xi \approx r_0P_0\lambda$. Assuming that the particulate and dissolved methane fluxes at the seafloor are negligible, Eq. (5) yields:

$$r_0P_0\lambda \approx F_{CH_4}(L) \tag{15}$$

Holmes *et al.* (2000) measured atmospheric methane fluxes $F_{CH_4}(L)$ of 1.4–1.7 μmol-CH_4/m^2-day at Station ALOHA (22°45′N, 158°0′W). These values were consistent with earlier measurements of 0.9–3.5 μmol-CH_4/m^2-day obtained by Tilbrook and Karl (1995) at Station ADIOS (26°0′N, 155°0′W). Emerson *et al.* (1997) evaluated the product $P_0\lambda$ at Station ALOHA (with λ = 100 m); the range was 1.64 to 4.65 mmol-C/m^2-day (0.6 to 1.7 mol-C/m^2-yr). This yields r_0 from 0.3 to 1 μmol-CH_4/mmol-C. Values of r measured at depths shallower than 150 m by Karl and Tilbrook (1994) at Stations ADIOS and VERTEX 4 (33°18′N, 139°6′W) range from 0.2 to 0.7. While this appears satisfactory, it should be noted that, according to our model, we should have $r \leq r_0$, the equality holding near the ocean surface. It is possible that the reduction in measured POC flux τ arising from

the use of a 335 μm mesh filter in sediment traps was not accompanied by a commensurate reduction in τ_{CH_4}. This would increase the value of r. If correct, this implies that methane-bearing particulate matter is more abundant in the form of smaller particles.

It is useful to verify that the particulate carbon sources discussed here are consistent with the formalism of current ecological models (e.g., Kawamiya *et al.,* 1995; Kishi *et al.,* 2001; Yanagi *et al.,* 2001). Zooplankton egestion P_{eg} typically is represented as a fraction γ of zooplankton grazing:

$$P_{eg} = \gamma G_{max}\{1 - \exp[k([Phy]^* - [Phy])]\}[Z] \tag{16}$$

where G_{max} is the maximum grazing rate, k the Ivlev constant, $[Phy]^*$ a threshold phytoplankton concentration and $[Z]$ the zooplankton concentration; G_{max} may depend on temperature, and Eq. (16) may be refined to distinguish between small zooplankton and large zooplankton, the latter being allowed to graze on both phytoplankton and small zooplankton. γG_{max} ranges between 0.2 and 0.4 per day. With $k = 0.47$ and $[Phy]^* = 0.1$ mg-Chl-a/m^3 (Yanagi *et al.,* 2001), and $[Phy]$ between 0.1333 (20/150) and 0.1666 (25/150) mg-Chl-a/m^3 for the latitudes of interest (Suzuki *et al.,* 1997), $\{1 - \exp[k([Phy]^* - [Phy])]\}$ typically varies from 0.0366 to 0.0645.

While P_{eg} ultimately may represent the methane-bearing POC source, P_0 as estimated by sediment trap measurements also includes the effect of phytoplankton and zooplankton mortality. For relatively warm surface waters, and $[Z]$ expressed in mmol-N/m^3, the mortality source P_{mo} is about 0.2 to 0.3 times $[Z]^2$ (Kawamiya *et al.,* 1995; Kishi *et al.,* 2001; Yanagi *et al.,* 2001). Assuming a molar ratio of organic nitrogen over organic carbon of 16/106, we should have:

$$P_{eg} + P_{mo} = (16/106)P_0. \tag{17}$$

Eq. (17) can be regarded as a second-degree polynomial in $[Z]$. Using previous ranges for the coefficients in P_{eg} and P_{mo}, and taking P_0 between 0.0164 to 0.093 mmol-C/m^3-day, from Emerson *et al.* (1997) with λ equal to 100 m or 50 m, respectively, one obtains a range for $[Z]$ between 0.06 and 0.25 mmol-N/m^3. It can be inferred from Evans and Parslow (1985) that in areas where phytoplankton concentrations $[Phy]$ do not vary extensively, herbivore concentrations are in quasi-equilibrium and range between one to four times $[Phy]$ (with the maximum during the summer months). Considering $[Z]$ to consist mostly of herbivores and with the previous range for $[Phy]$ (in mmol-N/m^3), this would yield a range for $[Z]$ between 0.08 and 0.42 mmol-N/m^3, in reasonable agreement with the result from Eq. (17).

b. Particulate fluxes

The solution of Eq. (7) and of Eq. (10) yields $p(x; \xi)$ and $p_{CH_4}(x; \xi)$, respectively. The corresponding fluxes are simply obtained from their definition, Eq. (1). The carbon problem requires that the production function P, and $\bar{X}$ be specified. For methane, the

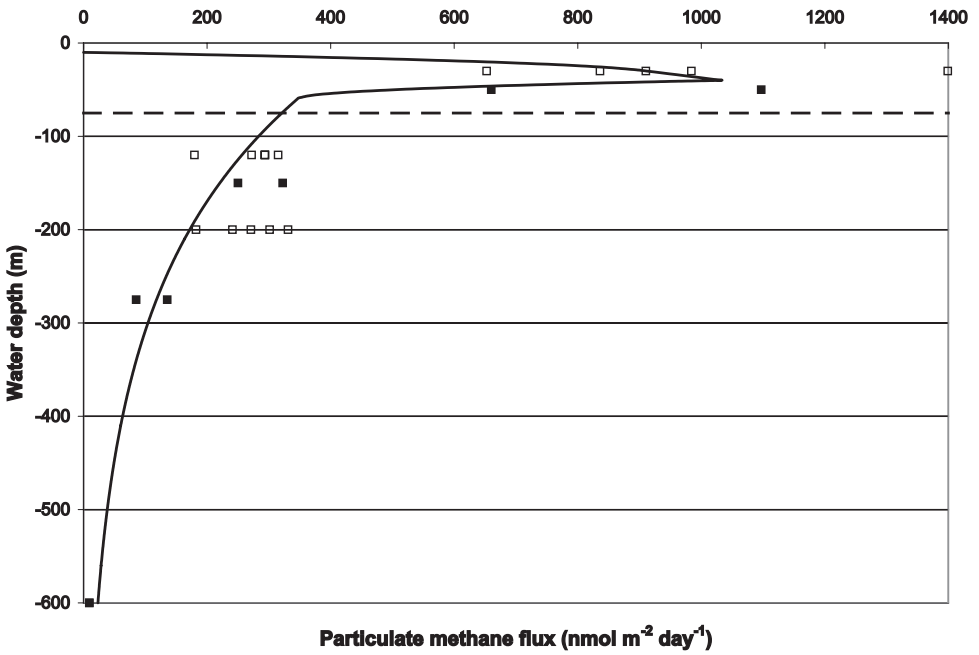

Figure 2. Particulate methane flux predictions with production P between 10 and 40 m depths (λ = 30 m), based on $F_{CH_4}(L) = 2.5$ μmol-CH_4 m^{-2} day^{-1} and $r_0 = 1$ μmol-CH_4/mmol-C, and $\bar{x}$ = 20 m, $\eta = 0.85$ and $\bar{X} = 200$ m; data from Karl and Tilbrook (1994) and Tilbrook and Karl (1995) at Stations ADIOS (open squares) and VERTEX 4 (filled squares)

additional input of r_0, $\bar{x}$ and η is necessary. If P is assumed constant over a layer of thickness λ, then the product $r_0 P$ is approximately $F_{CH_4}(L)/\lambda$.

Results were compared to the particulate data of Karl and Tilbrook (1994) and Tilbrook and Karl (1995) collected at Stations ADIOS and VERTEX 4. Accordingly, the time-average of the ocean-atmosphere flux reported by Tilbrook and Karl (1995) at Station ADIOS was used, i.e., $F_{CH_4}(L) = 2.5$ μmol-CH_4 m^{-2} day^{-1}. r_0 was taken as 1 μmol-CH_4/mmol-C. All things being equal, increasing $\bar{X}$ generates larger particulate fluxes at depths well below the production zone; decreasing η or increasing $\bar{x}$ globally increases particulate methane fluxes, since they correspond to a slower transfer to the water column; particulate methane fluxes also are proportional to r_0; finally, the value of λ determines P and completes the solution. A satisfactory representation of the particulate data was obtained with a shallow production zone between 10 and 40 m water depths (i.e., λ = 30 m), $\bar{X}$ = 200 m, $\bar{x}$ = 20 m and $\eta = 0.85$. Appendix A provides a general discussion of how measured profiles of POC concentrations or fluxes can help in estimating $\bar{X}$ as well as the water depth of the bottom of the POC producing layer. Figure 2 shows particulate methane fluxes and Figure 3 particulate carbon fluxes.

According to the present model, methane is released in particulate form (e.g., fecal

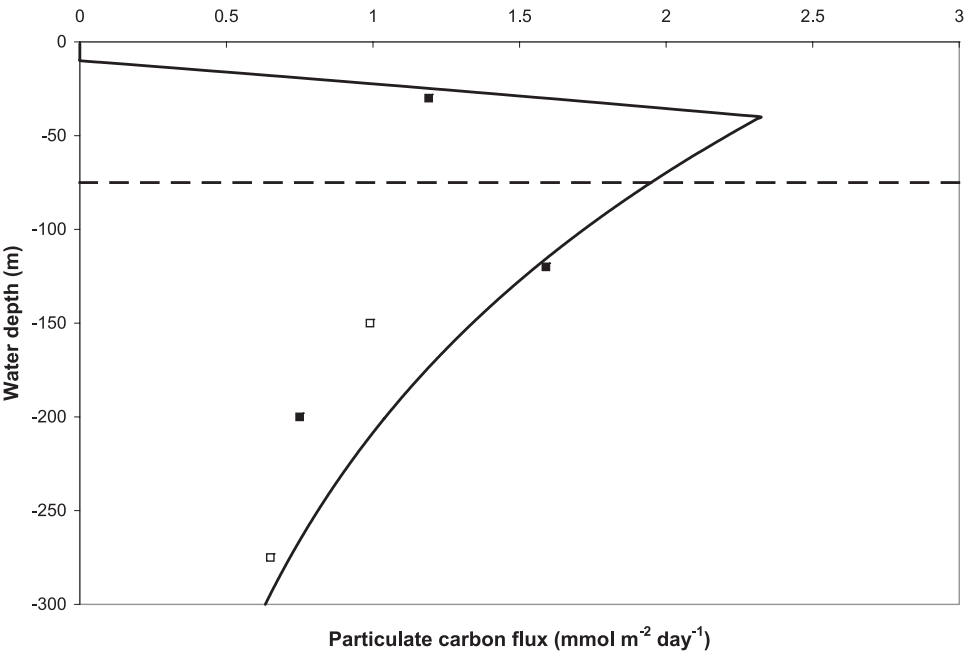

Figure 3. Particulate carbon flux predictions with production P between 10 and 40 m depths (λ = 30 m), based on $F_{CH_4}(L) = 2.5$ μmol-CH_4 m^{-2} day^{-1} and $r_0 = 1$ μmol-CH_4/mmol-C, and $\overline{X}$ = 200 m; data from Karl and Tilbrook (1994) and Tilbrook and Karl (1995) at Stations ADIOS (open squares) and VERTEX 4 (filled squares)

pellets) from a narrow layer close to the surface. Most of it is transferred to the water column within the mixed layer, and then into the atmosphere. As will be confirmed in the next Section, only a relatively small portion of the inferred methane production is necessary (and sufficient) to sustain concentrations and fluxes observed below the mixed layer.

c. Methane concentrations in the absence of oxidation

If Eq. (15) is used in the process of solving the particulate methane problem, methane oxidation is implicitly neglected. It was therefore consistent to first solve Eq. (11) with α = 0. The methane concentration data selected as reference consists of the four seasonal profiles obtained at Station ALOHA by Holmes *et al.* (2000). Corresponding ocean-atmosphere fluxes and average mixed-layer concentrations are shown in Table 1. For each data set, the particulate methane problem was solved with the parameters selected in Section 3.b and the appropriate input value $F_{CH_4}(L)$. The source function S_{CH_4} then could be derived via Eq. (3). Choices for the seafloor boundary condition u_0 are listed in Table 1. Eq. (11) subject to the two boundary conditions u_0 and u_m was solved either with constant vertical advection w or with the profile $w(x)$ discussed in Section 2c. K and either w

Table 1. Boundary values and parameters in methane concentration model.[1,2]

Month	October	January	April	July
$F_{CH_4}(L)$ (μmol-CH_4 m^{-2} day^{-1})	1.6	1.7	1.6	1.4
u_m (nM)	2.9	2.4	2.5	2.4
u_0 (nM)	0.8	0.5	0.5	0.5
Constant upward advection				
K (cm^2/s)	0.85	1.0	0.85	0.85
w (m/s $\times$ 10^7)				
$\alpha = 0$	5.25	6.0	5.5	5.25
$\alpha = 4.1 \times 10^{-5}$ day^{-1}	3.0			
$\alpha = 6.5 \times 10^{-5}$ day^{-1}	1.5			
Variable vertical advection[3]				
K (cm^2/s)	0.85	0.85	0.85	0.85
w_{tr} (m/s $\times$ 10^7)				
$\alpha = 0$	6.0	7.0	6.0	6.0
$\alpha = 4.1 \times 10^{-5}$ day^{-1}	3.0			

[1] $F_{CH_4}(L)$ and u_m from Holmes *et al.* (2000).
[2] In all cases, there is no methane oxidation below 1000 m depth.
[3] In all cases, $w_e = -1.0 \times 10^{-6}$ m/s, $H_{up} = 500$ m.

(constant advection) or w_{tr} (variable advection) were selected to yield a solution u in good agreement with the data. These parameters are listed in Table 1, and Figure 4 shows the corresponding methane concentration calculations for October 1996.

Results obtained with either constant or variable vertical advection rates are practically indistinguishable, except for January. Not surprisingly, K is lower than zero-advection values such as 1.8 cm^2/s proposed by Li *et al.* (1984); it also falls below 'historical' values (e.g., 1.4 cm^2/s in Munk, 1966), but is in good agreement with some recent estimates (0.85 cm^2/s in Hodnett and McNamara, 2000). The advection rates necessary to obtain a decent match with the data, however, are substantially higher than expected. Published estimates of w for constant-coefficient advection-diffusion models are of the order of 1.4×10^{-7} m/s (Munk, 1966). Similarly, values of w_{tr} suggested from the literature (e.g., Huang, 1992; Hodnett and McNamara, 2000) are about 3.0×10^{-7} m/s. These more credible choices for w or w_{tr} would yield excessive methane concentrations. The advective term $w(du/dx)$ in the left-hand-side of Eq. (11) is generally positive so that it behaves like a sink. Thus, the need for unrealistically large advection rates when solving Eq. (11) with $\alpha = 0$ indicates the relative importance of the omitted oxidation process.

d. Methane concentrations with oxidation

Specific methane oxidation rates α of the order of 4×10^{-5} per day were reported for the surface (aerated) layer of the Cariaco Basin (Ward *et al.,* 1987). This corresponds to turnover times of a little less than 70 years. In comparing the penetration of atmospheric methane and CFC11 in the northern Atlantic, Rehder *et al.* (1999) more recently estimated

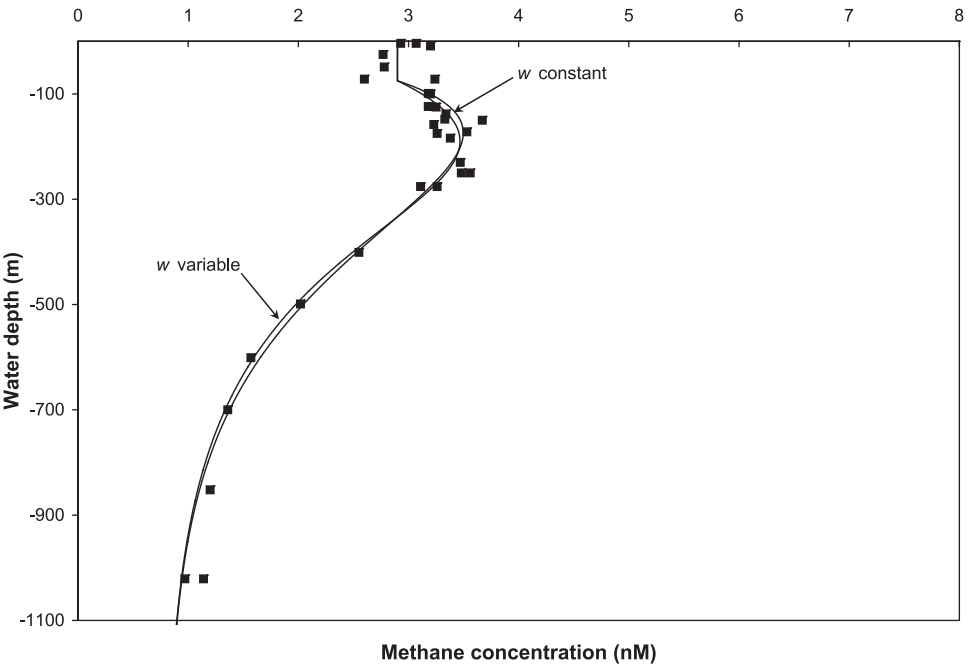

Figure 4. Calculated methane concentration profiles (no oxidation) and October 1996 data (■; Holmes *et al.,* 2000)

α to be 0.02 per year (5.5×10^{-5} per day). These relatively small values are representative of open ocean conditions and are consistent with the present model, although much faster oxidation rates with turnover times of only months have been observed (Ward and Kilpatrick, 1993; Valentine *et al.,* 2001) in areas affected by methane seafloor sources (from seeps and hydrate dissociation). In the close vicinity of methane-rich hydrothermal plumes, turnover times may drop even further with reported values of about a week (Cowen *et al.,* 2002).

If oxidation takes place throughout the entire open-ocean water column with $\alpha \approx 4 \times 10^{-5}$ per day, then the integrated strength of the oxidation sink is about 0.2 μmol-CH_4 m^{-2} day^{-1}. Particulate methane production must be greater by this amount, i.e., $\int_0^L \alpha u dx$ must be added in the right-hand-sides of Eq. (5) and Eq. (15). It is a matter open to discussion whether the increase would correspond to a change in P_0, r_0, or λ. In the case of Figures 2 and 3, for example, where $F_{CH_4}(L) = 2.5$ μmol-CH_4 m^{-2} day^{-1}, an 8% (0.2/2.5) increase of r_0 would leave the particulate-carbon fluxes shown in Figure 3 unchanged, and yield particulate methane fluxes in slightly better agreement with data. The addition of $\int_0^L \alpha u dx$ in Eq. (5) and Eq. (15) reflects further coupling between the particulate and dissolved methane problems. An efficient approach is to use a reasonable estimate of $\int_0^L \alpha u dx$, and separately solve the two problems, as done earlier. An iterative scheme could then be implemented if needed. Assuming that the particulate methane

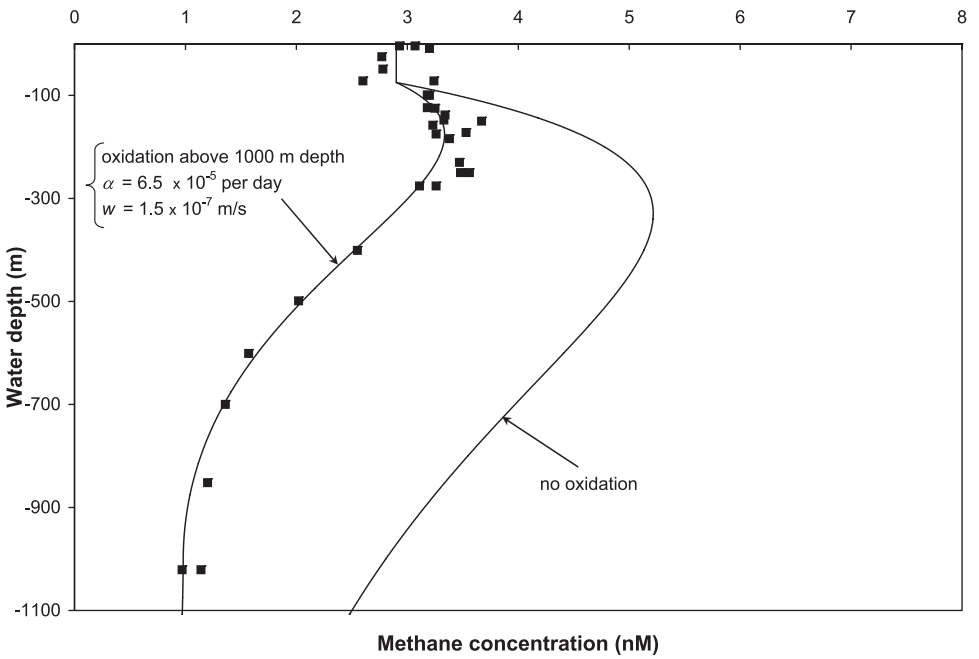

Figure 5. Methane concentration profiles with methane oxidation, $w = 1.5 \times 10^{-7}$ m/s and October 1996 data (■; Holmes *et al.,* 2000)

source adjustment is via higher r_0, with little loss of generality, the previous results for τ_{CH_4}, S_{CH_4}, etc. from Section 3.b remain applicable if simply multiplied by $\{F_{CH_4}(L) + \int_0^L \alpha u dx\}/F_{CH_4}(L)$. In particular, the modified function S_{CH_4} must be used in Eq. (11).

The October 1996 data of Holmes *et al.* (2000) was selected for model calculations with oxidation (nonzero α). Corresponding parameters are listed in Table 1. In all cases, it was necessary to postulate that oxidation ceases below a depth of about 1000 m; this is consistent with suggestions from Scranton and Brewer (1978), who related abyssal methane concentrations and the ages of deep water masses, and with observations that in the area of interest, methane concentrations do not significantly change below 800 m (Holmes *et al.,* 2000). Without a depth restriction on oxidation, the mathematical solution of Eq. (11) with realistic values of the oxidation rate would continue decreasing to near-zero concentrations (at around 2000 m depth) before increasing again to satisfy the seafloor boundary value. The correction of S_{CH_4} reflecting the strength of the integrated methane oxidation sink was adjusted accordingly.

Figure 5 shows results for a constant upward advection of $w = 1.5 \times 10^{-7}$ m/s, and $\alpha = 6.5 \times 10^{-5}$ per day. Although not plotted, nearly identical methane concentrations were obtained with $w = 3.0 \times 10^{-7}$ m/s and $\alpha = 4.1 \times 10^{-5}$ per day. These four parameters define ranges that are compatible with published work. Figure 6 shows the most satisfactory agreement between calculations and data, for variable vertical advection

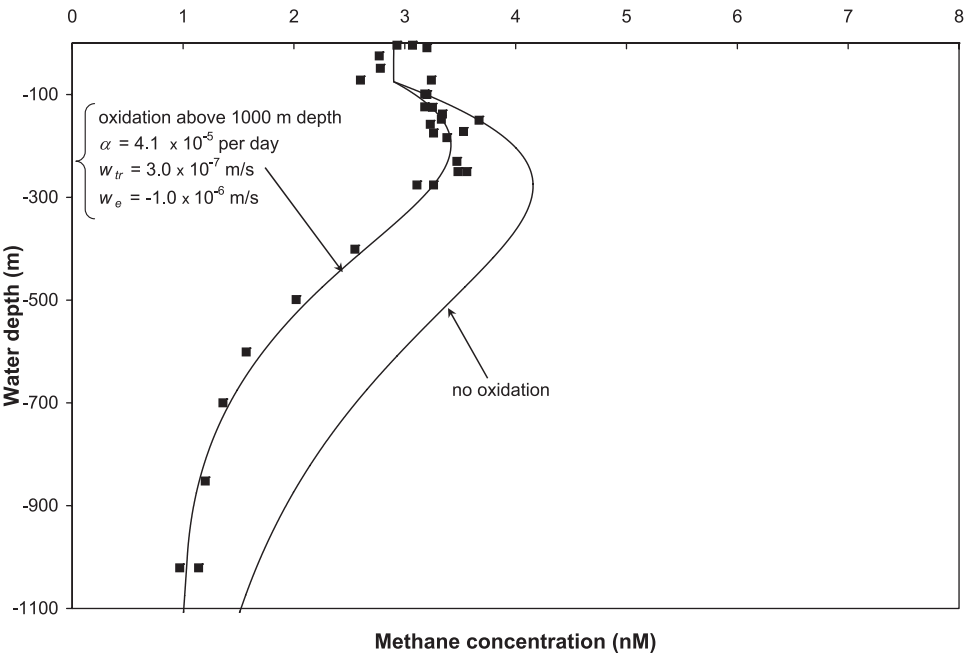

Figure 6. Methane concentration profiles with methane oxidation, $w_{tr} = 3.0 \times 10^{-7}$ m/s and October 1996 data (■; Holmes *et al.,* 2000)

($w_{tr} = 3 \times 10^{-7}$ m/s) and $\alpha = 4.1 \times 10^{-5}$ per day. These results correspond to the oxidation rate measured by Ward *et al.* (1987); vertical advection is moderately upward in the abyssal layer (at an average of 1.5×10^{-7} m/s in the bottom 3500 m), while Ekman pumping and subduction are represented by significant downward advection from the surface.

e. Isotopic composition

Eq. (14) was solved with the parameters corresponding to the concentration predictions shown in Figure 6 for the October 1996 data of Holmes *et al.* (2000). The upper boundary condition was the measured value of $\delta^{13}C$ in the mixed layer, $-45.6‰$. At the seafloor, an isotopic composition of the order of $-40‰$ was sought. Holmes *et al.* (2000) performed an isotopic budget of the upper ocean and estimated $\delta^{13}C_{new}$ to be about $-43‰$. Fractionation factors during methane oxidation were selected between 1.005 and 1.03 (Barker and Fritz, 1981; Coleman *et al.,* 1981).

Figure 7 shows calculated $\delta^{13}C$ and data. Measurements are relatively constant in the upper 300 m; substantial isotopic enrichment then occurs down to a depth of about 600 m; depletion progressively takes place in deeper waters. The existence of a maximum for $\delta^{13}C$ is predicted with the higher value $\alpha_k = 1.03$ at a depth of the order of 800 m, but $\delta^{13}C$ noticeably increases from the mixed layer downwards. With $\alpha_k = 1.005$, calculated

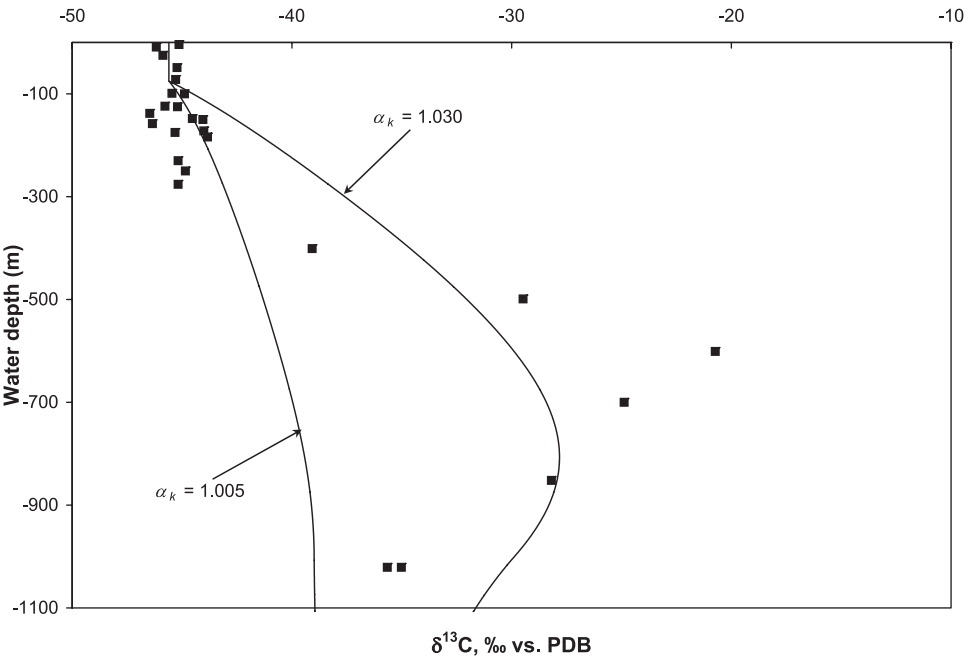

Figure 7. Isotopic composition profiles and October 1996 data (■; Holmes *et al.,* 2000)

isotopic compositions are closer to the data in the upper 300 m, but are significantly under predicted in the water column below.

With the present model, only unrealistic parametric combinations of low $\delta^{13}C_{new}$ (e.g. $-60‰$) and high oxidation fractionation factors (e.g. $\alpha_k = 1.05$) could bring a better overall agreement between calculated and measured isotopic compositions: a balance would be established between a very depleted source (low $\delta^{13}C_{new}$) and a very enriching process (high α_k) in the upper 300 m layer, where methane transfer from particulate matter is substantial; strong enrichment would take place underneath, until a maximum is reached when the relative effect of methane oxidation starts waning.

Limitations of the one-dimensional advection-diffusion model are expected to be magnified with $\delta^{13}C$ (the anomaly of an isotopic ratio). While isotopic analyses have become a tool of choice for investigating the global carbon biogeochemical cycle (e.g. Kelley *et al.,* 1998), their sensitivity is expected to promote (and require) the development of more complex transport models. As noted in Holmes *et al.* (2000), the very sharp enrichment measured at 600 m likely reflects the presence of modified North Pacific Intermediate Water (NPIW), which is older than waters both above and below. In Section 2.c, it was argued that in one-dimensional models, a variable upwelling $w(x)$ could incorporate the effects of subduction and lateral mixing to some extent. The consideration of pseudo-sources of water dw in elementary mass balances preserved the form of Eq. (11) as long as the associated pseudo-sources of tracers such as u were udw. If the variation in w

were to reflect lateral mixing with waters of 'markedly different characteristics', the pseudo-sources of associated tracers might have to be modified (e.g. $\bar{u}\mathrm{d}w$ instead of $u\mathrm{d}w$). A net source $(\bar{u} - u)(\mathrm{d}w/\mathrm{d}x)$ would then appear in the right-hand-side of Eq. (11). In the case of isotopic composition, this would suggest that isotopic fractionation may occur from advection.

4. Conclusions

Assuming that the methane found in large regions of open-ocean waters is of particulate origin, a simple one-dimensional physical model was developed. It was postulated that methane-bearing pellets were formed in a shallow layer close to the surface. The gravitational settling of this particulate matter was represented in the simplest way, with the rapid diffusion of most of the trapped methane. Pellets were allowed to degrade slowly during and following this initial phase. The methane transferred to the water column then provided the required source to a one-dimensional advection-diffusion model of methane concentrations. A constant eddy diffusion coefficient was considered below the mixed layer; vertical advection was either constant upwards, or varying with depth. Variable vertical advection rates allowed the representation of Ekman pumping (upper layer downwelling) and subduction.

Predicted carbon and methane particulate fluxes were in good agreement with available data, using model parameters that fell within expected orders of magnitude. The particulate methane production region appeared to be quite shallow (approximately 30 m thick), and well within the mixed layer. This would indicate that most particulate methane is transferred to the water column and to the atmosphere quite rapidly, with limited effects on oceanic methane concentration profiles below the mixed layer.

Even with the escape of most methane to the atmosphere, the water-column source proved to be significant below the mixed layer, but not strong enough to overwhelm methane oxidation. Without methane oxidation, vertical advection rates that provided a good match with the data of Holmes *et al.* (2000) collected in the central North Pacific Subtropical Gyre were much larger than expected. The inclusion of first-order methane oxidation with acceptable advection rates brought model predictions and data in close agreement, although known oxidation rates are very small with turnover times of several decades.

Predictions of the isotopic composition of dissolved methane $\delta^{13}C$ with the one-dimensional model seemed relatively less successful when published oxidation fractionation factors and particulate methane isotopic composition were used. Trends in measured $\delta^{13}C$ vertical profiles could be reproduced, however, with ^{13}C enrichment increasing downward to a maximum value at depths of a few hundred meters.

Acknowledgments. The authors are grateful to F. J. Sansone for providing them with the data sets reported in Holmes *et al.* (2000), and for a helpful discussion on the oceanic methane cycle. Funding for this study was provided by the Office of Naval Research through the Hawaii Energy and Environmental Technology Initiative.

APPENDIX

Estimation of the Particulate Degradation Length $\bar{X}$ and of the Water Depth of the Bottom of the POC Producing Layer from POC Data

This Appendix examines how the value $\bar{X} = 200$ m used in this paper to model specific particulate carbon and methane data sets (Karl and Tilbrook, 1994; Tilbrook and Karl, 1995) can be further constrained over time and space. Using Eq. (7) into Eq. (1), Eq. (2) and Eq. (3), the following expression may be derived for the POC flux τ.

$$\frac{d\tau}{dx} = \frac{\tau}{\bar{X}} - \mathrm{P(x)}$$

If the POC production function P is modeled as a constant P_0 through a near-surface layer of thickness λ, the solution of the above differential equation can easily be obtained. An example is shown as the curve in Figure 3. Qualitatively, the POC flux τ increases from the seafloor to the bottom of the POC producing layer, through a region where $P = 0$. It then starts decreasing across the POC producing layer, down to zero near the ocean surface. Between any two points x_1 and x_2 within the deeper region where $P = 0$, the following identity can be established:

$$\bar{X} = \frac{\mathrm{x_2 - x_1}}{\mathrm{Log}\left(\frac{\tau_2}{\tau_1}\right)} \tag{A1}$$

If measurements of the POC flux are available as a function of time for two water depths well below the inferred POC production layer, then Eq. (A1) is a point estimate of the characteristic particulate degradation length $\bar{X}$.

The Hawaii Ocean Time (HOT) series data has been collected mostly at Station ALOHA over many years (Karl and Lukas, 1996). It includes POC flux measurements at depths of 150 m and 300 m over the period December 1988 through May 1995 (HOT Cruises 2 through 63). This data was extracted using the Hawaii Ocean Time-series Data Organization and Graphical System (HOT-DOGS©) at http://hahana.soest.hawaii.edu/hot/hot-dogs/interface.html, and used with Eq. (A1) to estimate $\bar{X}$. Figure 8 shows the results where 10 outliers were discarded; a time-average value of 250 m and a standard deviation of 90 m were obtained, in reasonable agreement with the model selection of 200 m.

Profiles of the POC concentrations $[POC]$ from water bottle sampling represent a greater source of POC data than direct flux measurements. In the model, particulate sinking was assumed to dominate other transport mechanisms, so that $\tau = -W[POC]$. With the further assumption of a constant particulate sinking velocity $-W$, the proportionality between τ and $[POC]$ is uniform. In particular, Eq. (A1) can be reformulated as:

$$\bar{X} = \frac{\mathrm{x_2 - x_1}}{\mathrm{Log}\left(\frac{[\mathrm{POC}]_2}{[\mathrm{POC}]_1}\right)} \tag{A2}$$

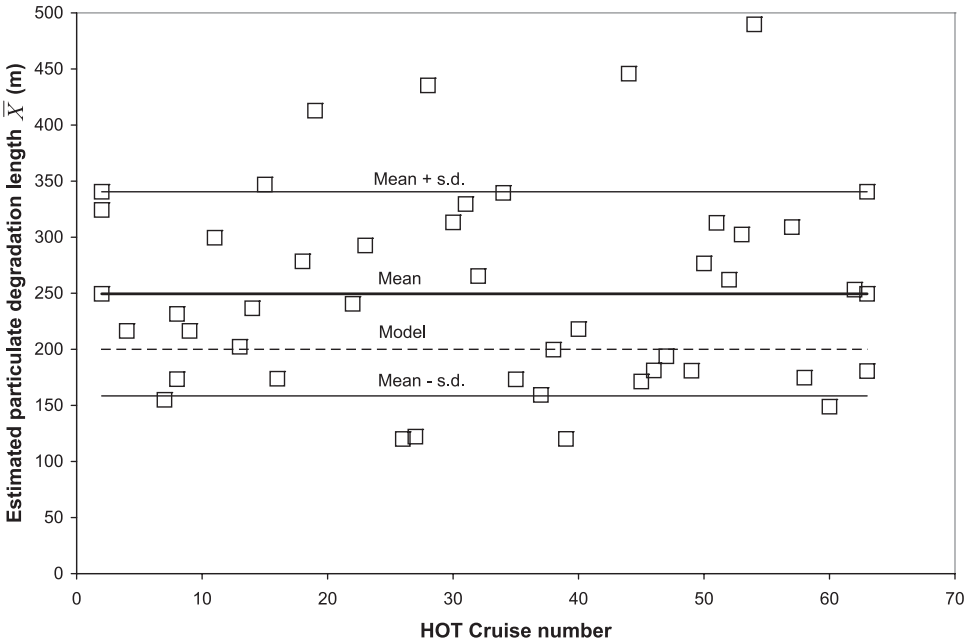

Figure 8. Particulate degradation length $\overline{X}$ as a function of time from POC fluxes at 150 m and 300 m depths (HOT data base)

To get a sense of geographic variability for $\overline{X}$, the $[POC]$ data of Burke *et al.* (1983) collected at nine Stations in the eastern tropical North Pacific (ETPN) was considered. The region surveyed extends from 25°N to equatorial latitudes and spans over 25 degrees in longitude. For each Station, the water depth of the $[POC]$ maximum was identified with the bottom of the POC producing layer. The average value of this depth for the nine Stations is 38 m with a standard deviation of 34 m, in good agreement with our selection of 40 m in the paper. At each Station, Eq. (A2) was used to estimate $\overline{X}$ by combining the $[POC]$ maximum with each $[POC]$ data point collected at a deeper water depth. Discarding 2 outliers, means $\pm$ one standard deviation obtained with this procedure are shown in Figure 9.

Finally, POC concentrations in the HOT data base were examined to further confirm our estimate of the water depth of the bottom of the POC producing layer. The $[POC]$ maximum was found to be at an average depth of 43 m, with a standard deviation of 25 m. Once more, this is in good agreement with the model selection of 40 m.

Notation

A	particulate degradation coefficient (day^{-1})
C_0	methane concentration in particulate matter (mol/m^3)
F	water-column flux (mol/m^2-day)

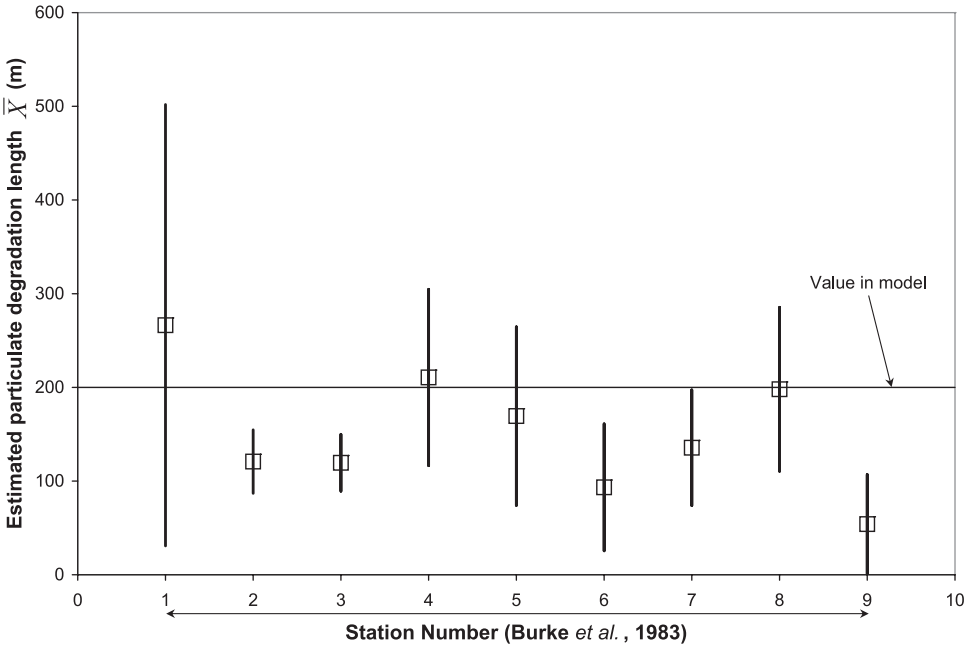

Figure 9. Particulate degradation length $\overline{X}$ as a function of location from POC concentration profiles (Burke *et al.,* 1983)

G_{max}	maximum zooplankton grazing rate (day^{-1})
H	mass transfer coefficient (m/day)
h_m	thickness of mixed layer (m)
H_{up}	thickness of water column above abyssal layer (m)
k	Ivlev constant (m^3/mg-Chl-a)
K	turbulent vertical diffusion coefficient (m^2/day)
L	ocean depth (m)
P	particulate production source (mol/m^3-day)
P_0	constant particulate production source (mol/m^3-day)
P_{eg}	zooplankton egestion source (mol/m^3-day)
P_{mo}	zooplankton mortality source (mol/m^3-day)
p	partial particulate source from settlement (mol/m^3-day)
$[Ph]$	phytoplankton concentration (mg-Chl-a/m^3)
$[Ph]^*$	threshold phytoplankton concentration (mg-Chl-a/m^3)
$[POC]$	Particulate Organic Carbon concentration (mol/m^3)
r	ratio of particulate methane flux over particulate carbon flux
r_0	initial value of r
R	isotopic ratio ^{13}C/^{12}C of methane
R_{new}	isotopic ratio of methane in particulate matter

R_{PDB}	isotopic ratio of PDB standard
s	particulate surface area production (m^{-1}-day^{-1})
S	water-column source of particulate origin (mol/m^3-day)
u	water-column methane concentration (mol/m^3)
u_m	mixed-layer methane concentration (mol/m^3)
u_0	seafloor methane concentration (mol/m^3)
^{13}u	water-column $^{13}CH_4$ concentration (mol/m^3)
$^{13}u_{ox}$	$^{13}CH_4$ concentration in methane removed by oxidizing bacteria (mol/m^3)
$\bar{u}$	auxiliary tracer concentration (mol/m^3)
W	sinking velocity of particulate matter (m/day)
w	constant upward advection rate (m/day)
w_e	vertical advection rate at ocean surface (m/day)
w_{tr}	vertical advection rate at top of abyssal layer (m/day)
x	vertical coordinate (m)
$\bar{x}$	particulate diffusive length scale (m)
$\bar{\bar{x}}$	particulate diffusive length scale adjusted for degradation (m)
$\overline{X}$	particulate degradation length scale (m)
$[Z]$	zooplankton concentration (mol/m^3)

Greek letters

α	methane oxidation rate (day^{-1})
α_k	isotopic fractionation for microbial methane oxidation
$\delta^{13}C$	isotopic composition (‰)
$\delta^{13}C_{new}$	isotopic composition of methane in particulate matter (‰)
γ	fraction of zooplankton grazing egested
η	fraction of dissolvable particulate methane
λ	depth of constant particulate production layer (m)
τ	particulate flux (mol/m^2-day)
ξ	auxiliary vertical coordinate (m)
χ	auxiliary vertical coordinate (m)

Subscripts

CH_4	related to methane

REFERENCES

Barker, J. F. and P. Fritz. 1981. Carbon isotope fractionation during microbial methane oxidation. Nature, *293,* 289–291.

Burke, A. J., Jr., D. F. Reid, J. M. Brooks and D. M. Lavoie. 1983. Upper water column methane geochemistry in the eastern tropical North Pacific. Limnol. Oceanogr., *28,* 19–32.

Coleman, D. D., J. B. Risattiand and M. Schoell. 1981. Fractionation of carbon and hydrogen isotopes by methane-oxidizing bacteria. Geochim. Cosmochim. Acta, *45,* 1033–1039.

Conrad, R. and W. Seiler. 1988. Methane and hydrogen in seawater (Atlantic Ocean). Deep Sea Res., *35,* 1903–1917.

Cowen, J. P., X. Wen and B. N. Popp. 2002. Methane in aging hydrothermal plumes. Geochim. Cosmochim. Acta, *66,* 3563–3571.

Craig, H. 1957. Isotopic standards for carbon and oxygen and correction factors for mass spectrometric analysis of carbon dioxide. Geochim. Cosmochim. Acta, *12,* 133–149.

Dietrich, W. E. 1982. Settling velocity of natural particles. Water Resour. Res., *18,* 1615–1626.

Emerson, S., P. Quay, D. Karl, C. Winn, L. Tupas and M. Landry. 1997. Experimental determination of the organic carbon flux from open-ocean surface waters. Nature, *389,* 951–954.

Evans, G. T. and J. S. Parslow. 1985. A model of annual plankton cycles. Biol. Oceanogr., *3,* 327–347.

Flament, P., S. Kennan, R. Lumpkin, M. Sawyer and E. Stroup. 1997. The Ocean Atlas of Hawai'i, poster from the Satellite Oceanography Laboratory, School of Ocean and Earth Science and Technology, University of Hawai'i, http://www.satlab.hawaii.edu/atlas/.

Hodnett, P. F. and R. McNamara. 2000. A modified Stommel-Arons model of the abyssal ocean circulation. Math. Proc. Royal Irish Ac., *100A,* 85–104.

Holmes, M. E., F. J. Sansone, T. M. Rust and B. N. Popp. 2000. Methane production, consumption, and air-sea exchange in the open ocean: An evaluation based on carbon isotopic ratios. Global Biogeochem. Cycles, *14,* 1–10.

Huang, R. X. 1992. A two-level model for the wind and buoyancy-forced circulation. J. Phys. Oceanogr., *23,* 104–115.

IPCC. 2001. Climate Change 2001: The Scientific Basis. Cambridge University Press, Cambridge, England, 944 pp.

Jumars, P. A., D. L. Penry, J. A. Baross, M. J. Perry and B. W. Frost. 1989. Closing the microbial loop: dissolved carbon pathway to heterotrophic bacteria from incomplete ingestion, digestion and absorption in animals. Deep-Sea Res., *36,* 483–495.

Karl, D. M. and R. Lukas. 1996. The Hawaii Ocean Time-series (HOT) program: Background, rationale and field implementation. Deep-Sea Res. II, *43,* 129–156.

Karl, D. M. and B. D. Tilbrook. 1994. Production and transport of methane in oceanic particulate organic matter. Nature, *368,* 732–734.

Kawamiya, M., J. Kishi, Y. Yamanaka and N. Suginohara. 1995. An ecological-physical coupled model applied to Station Papa. J. Oceanogr., *51,* 635–664.

Kelley, C. A., R. B. Coffin and L. A. Cifuentes. 1998. Stable isotope evidence for alternative bacterial carbon sources in the Gulf of Mexico. Limnol. Oceanogr., *43,* 1962–1969.

Kishi, M. J., H. Motono, M. Kashiwai and A. Tsuda. 2001. An ecological-physical coupled model with ontogenetic vertical migration of zooplankton in the Northwestern Pacific. J. Oceanogr., *57,* 499–507.

Li, Y. H., T. H. Peng and W. S. Broecker. 1984. The average vertical mixing coefficient for the oceanic thermocline. Tellus, *36B,* 212–217.

MacDonald, A. M. and C. Wunsch. 1996. An estimate of global ocean circulation and heat fluxes. Nature, *382,* 436–439.

Munk, W. H. 1966. Abyssal recipes. Deep Sea Res., *13,* 707–730.

Pierce, D. W. 2004. Future changes in biological activity in the North Pacific due to anthropogenic forcing of the physical environment. Clim. Change, *62,* 389–418.

Reeburgh, W. S. 2003. Global methane biogeochemistry, *in* Treatise on Geochemistry, H. D. Holland and K. K. Turekian, eds., 65–89.

Rehder, G., R. S. Keir and E. Suess. 1999. Methane in the Northern Atlantic controlled by microbial oxidation and atmospheric history. Geophys. Res. Lett., *26,* 587–590.

Sansone, F. J., B. N. Popp, A. Gasc, A. W. Graham and T. M. Rust. 2001. Highly elevated methane in

the eastern tropical North Pacific and associated isotopically enriched fluxes to the atmosphere. Geophys. Res. Lett., *28,* 4567–4570.

Scranton, M. I. and P. G. Brewer. 1978. Consumption of dissolved methane in the deep ocean. Limnol. Oceanogr., *23,* 1207–1213.

Stommels, H. 1958. The abyssal circulation. Deep-Sea Res., *5,* 80–82.

Suzuki, K., N. Handa, H. Kiyosawa and J. Ishizaka. 1997. Temporal and spatial distribution of phytoplankton pigments in the central Pacific Ocean along 175°E during the boreal summers of 1992 and 1993. J. Oceanogr., *53,* 383–396.

Tilbrook, B. D. and D. M. Karl. 1995. Methane sources, distributions and sinks from California coastal waters to the oligotrophic north Pacific gyre. Mar. Chem., *49,* 51–64.

Valentine, D. L., D. C. Blanton, W. S. Reeburgh and M. Kastner. 2001. Water column methane oxidation adjacent to an area of active hydrate dissociation, Eel River Basin. Geochim. Cosmochim. Acta, *65,* 2633–2640.

Ward, B. B. and K. A. Kilpatrick. 1993. Methane oxidation associated with mid-depth methane maxima in the Southern California Bight. Cont. Shelf Res., *13,* 1111–1122.

Ward, B. B., K. A. Kilpatrick, P. C. Novelli and M. I. Scranton. 1987. Methane oxidation and methane fluxes in the ocean surface layer and deep anoxic waters. Nature, *327,* 226–229.

Watanabe, S., N. Higashitani, N. Tsurushima and S. Tsunogai. 1995. Methane in the Western North Pacific. J. Oceanogr., *51,* 39–60.

Winn, C. D., F. T. Mackenzie, C. J. Carillo, C. L. Sabine and D. M. Karl. 1994. Air-sea carbon dioxide exchange in the North Pacific Subtropical Gyre: Implications for the global carbon budget. Global Biogeochem. Cycles, *8,* 157–163.

Yanagi, T., G. Onitsuka, N. Hirose and J. H. Yoon. 2001. A numerical simulation on the mesoscale dynamics of the spring bloom in the Sea of Japan. J. Oceanogr., *57,* 617–630.

Received: *24 October 2005;* revised: *3 May, 2006.*